Pulsed laser photolysis kinetics study of the O(3 P)+ClO reaction

J. M. Nicovich, P. H. Wine, and A. R. Ravishankara

Citation: The Journal of Chemical Physics **89**, 5670 (1988); doi: 10.1063/1.455574
View online: http://dx.doi.org/10.1063/1.455574
View Table of Contents: http://scitation.aip.org/content/aip/journal/jcp/89/9?ver=pdfcov
Published by the AIP Publishing

Pulsed laser photolysis kinetics study of the $O(^3P)+ClO$ reaction

J. M. Nicovich, P. H. Wine,[a] and A. R. Ravishankara[b]
Molecular Sciences Branch, Georgia Tech Research Institute, Georgia Institute of Technology, Atlanta, Georgia 30332

(Received 23 June 1988; accepted 21 July 1988)

A pulsed laser photolysis technique has been employed to study the kinetics of the important stratospheric reaction $O + ClO \xrightarrow{k_1} Cl + O_2$ in N_2 buffer gas over the temperature and pressure ranges 231–367 K and 25–500 Torr. 351 nm pulsed laser photolysis of $Cl_2/O_3/N_2$ mixtures produced Cl atoms in excess over O_3. After a delay sufficient for the reaction $Cl + O_3 \rightarrow ClO + O_2$ to go to completion, a small fraction of the ClO was photolyzed at 266 nm to produce $O(^3P)$. The decay of $O(^3P)$ in the presence of an excess, known concentration of ClO was then followed by time-resolved resonance fluorescence spectroscopy. We find that k_1 is independent of pressure, but that $k_1(T)$ increases with decreasing temperature. Our results suggest that the Arrhenius expression $k_1(T) = (1.55 \pm 0.33) \times 10^{-11} \exp\{(263 \pm 60)/T\}$ cm^3 $molecule^{-1}$ s^{-1} is appropriate for modeling stratospheric chemistry. Errors in the Arrhenius expression are 2σ and represent precison only. The absolute accuracy of k_1 at any temperature within the range studied is estimated to be $\pm 20\%$. Our results agree with other recent measurements of k_1 at 298 K but give significantly faster rate coefficients at stratospheric temperatures. A few measurements of the rate coefficient for the reaction $ClO + ClO \xrightarrow{k_7}$ products were also carried out. These measurements were necessary to assess the time dependence of [ClO].

INTRODUCTION

The reaction of ground state oxygen atoms $O(^3P)$ with ClO radicals is the rate determining step in the dominant catalytic cycle via which chlorine atoms destroy odd oxygen in the middle stratosphere:

$$O + ClO \rightarrow O_2 + Cl, \quad (1)$$

$$Cl + O_3 \rightarrow ClO + O_2 \quad (2)$$

$$\text{Net: } O + O_3 \rightarrow 2O_2 .$$

The primary source of stratospheric chlorine atoms is the photolysis of anthropogenic chlorofluorocarbons.

Seven measurements of $k_1(298\text{ K})$ are reported in the literature.[1-7] There is agreement among the five most recent studies that $k_1(298\text{ K})$ lies in the range $3.5\text{–}4.2 \times 10^{-11}$ cm^3 $molecule^{-1}$ s^{-1}. The activation energy for reaction (1) is known to be small,[2-7] but its value is not as well defined as would be desirable for such an important stratospheric reaction. In fact, it is not clear if $k_1(T)$ increases or decreases with decreasing temperature. In addition to the abovementioned studies of reaction (1) at atmospheric temperatures, one high temperature (1250 K) shock tube measurement of k_1 has been reported,[8] as has one theoretical calculation of $k_1(T)$ over the temperature range 220–1000 K.[9]

Because predictions of chlorine catalyzed ozone loss are very sensitive to the value of $k_1(T)$ used in model calculations, it is important that this rate coefficient be determined with high precision at stratospheric temperatures. Studies employing a variety of experimental techniques are desirable in order to uncover possible systematic errors. All previous studies of reaction (1) at ambient and subambient temperatures[1-7] employed discharge flow systems which were limited to total pressures of 10 Torr or less. It is interesting to note that reaction (1) occurs on a potential energy surface with a minimum along the reaction coordinate, i.e., the intermediate complex ClOO is a bound species whose ground state correlates with $O(^3P) + ClO(X\,^2\pi)$.[10] Reactions which occur on potential energy surfaces of this type often exhibit negative activation energies and pressure dependent rates.

We have recently developed a pulsed laser photolysis method for carrying out direct kinetics studies of radical–radical reactions at pressures up to 1 atm, and applied this method to study the temperature and pressure dependences of the $O + HO_2$ reaction.[11,12] Using an extension of the technique employed in the $O + HO_2$ investigations, we have studied the kinetics of reaction (1) in N_2 buffer gas over the temperature and pressure ranges 231–367 K and 25–200 Torr. Our results, which include observation of a significant negative activation energy, are reported in this paper.

EXPERIMENTAL

A schematic of the apparatus appears in Fig. 1. The two radical species were created via a scheme involving two separate photolysis lasers. Under "slow flow" conditions, a gas mixture containing Cl_2 and O_3 in a large excess of N_2 buffer gas was first subjected to photolysis by a XeF excimer laser,

$$Cl_2 + h\nu(351\text{ nm}) \rightarrow 2Cl. \quad (3)$$

[a] Author to whom correspondence should be addressed.
[b] Present address: Aeronomy Laboratory, National Oceanic and Atmospheric Administration, 325 Broadway, Boulder, CO 80303.

 0021-9606/88/215670-10$02.10

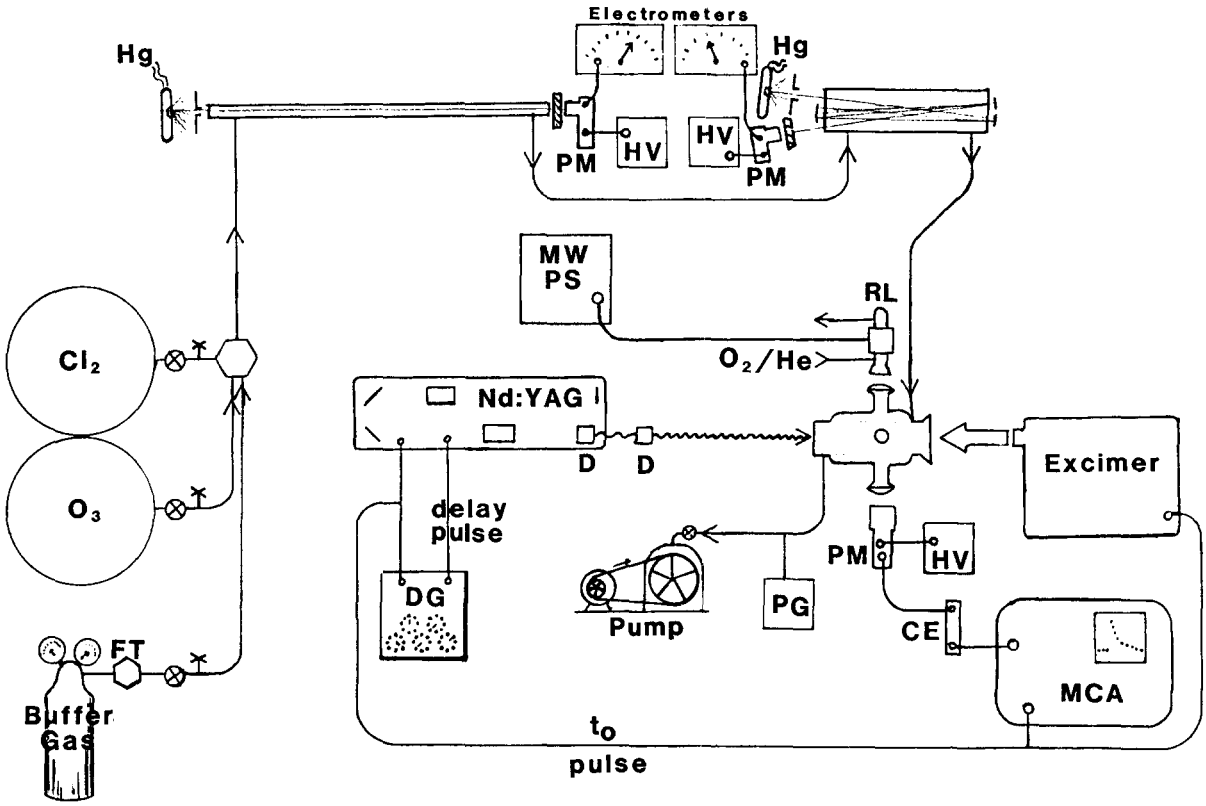

FIG. 1. Schematic diagram of the experimental apparatus. The abbreviations used are as follows: FT—flow transducer; Hg—mercury pen-ray lamp; PM—photomultiplier tube; HV—high voltage power supply; MWPS—microwave power supply; RL—resonance lamp; DG—delay generator; PG—pressure gauge; MCA—multichannel analyzer; D—doubling crystal; CE—counting electronics. For the sake of clarity, the resonance lamp and photomultiplier tube are shown facing each other when, in fact, they were mounted at 90° to each other and perpendicular to the direction of the laser beams.

The combination of the excimer laser fluence and $[Cl_2]$ was always large enough for the condition $[Cl]_0 > [O_3]_0$ to hold. During a predetermined delay period, t_d, the reaction

$$Cl + O_3 \rightarrow ClO + O_2 \qquad (2)$$

was allowed to go to completion. At this time the ozone in the reaction cell had effectively been titrated by Cl atoms and the initial value of $[O_3]_0$ could be related to $[ClO]_{t_d}$. At the end of this delay a second laser pulse, the fourth harmonic of the fundamental wavelength from a Nd:YAG laser, photolyzed a small fraction of the ClO,

$$ClO + h\nu(266\ \text{nm}) \rightarrow Cl + O. \qquad (4)$$

The decay of oxygen atoms in the presence of excess ClO was followed by monitoring the time dependence of fluorescence signal which was continuously excited by a microwave discharge resonance lamp. The lamp was operated with a low pressure of helium (<1 Torr) containing a small fraction of O_2.

The ozone storage bulb contained a mixture of 1% to 2% O_3 in nitrogen, while the Cl_2 was stored neat. These species were leaked through needle valves into the main gas flow. Ozone in the gas flow was measured in a 35.0 cm absorption cell that was placed within a multipass optical arrangement. Using modified White cell optics, 30 passes of the 254 nm Hg line from a pen-ray lamp were sent through the absorption cell for an effective path length of 10.50 m. The chlorine was measured in a 216 cm absorption cell using a single pass of the 366 nm Hg line, also from a pen-ray lamp. Both atomic lines were isolated using suitable bandpass filters. Typically, the absorption cells were upstream from the reaction cells, although in a few experiments the Cl_2 and O_3 were measured after the flow exited the reaction cell. Because Cl_2 absorbance at 254 nm was not totally negligible [$\sigma = 1.6\times10^{-21}$ cm^2 (Ref. 13)], the reference light intensity for the $[O_3]$ determination was always measured with Cl_2 flowing. The Cl_2 absorption cross section at 366 nm and the O_3 absorption cross section at 254 nm were taken to be 1.01×10^{-19} cm^2 (Ref. 13) and 1.147×10^{-17} cm^2 (Ref. 14), respectively.

The Pyrex reaction cell measured 16 cm along its longer axis and had an internal diameter of 4 cm. The two laser beams counterpropagated along the longer axis. Around the middle of the cell were four 1.5 cm diameter side arms, each perpendicular to the long axis of the cell and at 90° to each other. The resonance lamp radiation entered the cell through one of the side arms and the fluorescence signal was collected through a neighboring arm. The central portion of the cell was surrounded by a jacket through which thermostated liquids were flowed to control the temperature of the

gas mixture inside the reactor. The gas mixture entered the cell through several ports very near the window at one end of the long axis and exited the cell through similar ports near the opposite window. Because the chemistry initiated by the excimer laser beam completely titrated one component (O_3) of the gas mixture within much of the cell volume, the cell was designed to have minimum total volume and low dead space, i.e., gas flowed through all volume elements of the cell at approximately equal rates. The typical linear flow rate through the cell was 14 cm s^{-1} and the repetition rate of the two laser sequence was usually 0.4 Hz. Therefore, the gas mixture within the entire volume of the reaction cell was replenished between excimer laser pulses. The temperature of the gas mixture was measured by replacing one of the end windows with an acrylic flange through which a copper–constantan thermocouple could be inserted. The errors in the reported temperatures are estimated to be no more than $\pm$ 1.0 K at the extreme temperatures and less at intermediate temperatures.

Oxygen resonance lamp radiation was focused into the reaction zone by a 2 in. focal length MgF_2 lens. The reaction zone was viewed by a solar blind photomultiplier tube through a similar lens. The volumes between the resonance lamp and the reaction cell, and between the reaction cell and the photomultiplier tube were purged with a mixture of 1% O_2 in nitrogen. This excluded room air and also acted as a filter of extraneous emissions from the resonance lamp. A CaF_2 window between the cell and the photomultiplier tube eliminated the possibility of hydrogen atom detection. Fluorescence signals were accumulated using photon counting techniques in conjunction with multichannel scaling. Each sweep of the analyzer was triggered simultaneously with the excimer laser. From 50 to 500 flashes were averaged to obtain sufficient signal-to-noise ratio for quantitative kinetic analysis.

The total pressure in the flow system was measured with a capacitance manometer. Due to the necessarily fast flow rate and the small (4.0 mm i.d.) tubing connecting the various components of the flow system, there were measurable pressure gradients between the absorption cells and the reaction cell. Quantitative adjustments were made for these gradients in the calculation of the Cl_2 and O_3 concentrations in the reaction cell under each set of conditions. The magnitude of the adjustment was largest at the lowest pressure (15% at 25 Torr) and negligible at the highest (1% at 200 Torr). The nitrogen buffer gas comprised at least 94% of the mixture for all experiments and its flow rate was monitored using a calibrated electronic mass flowmeter.

The concentration of ClO, the excess species in this technique, was derived from the concentration of ozone as measured "*in situ*." Therefore, it was not necessary to have an absolute calibration of the photolysis laser fluences. However, it was important to know that following the excimer laser pulse the condition $[Cl] > [O_3]$ held throughout the reaction zone. Therefore, the excimer laser fluence was measured in each experiment. As will be discussed below, it was also important to monitor the 266 nm laser fluence. Both of these quantities were determined using a photodiode-based calibrated radiometer. With the front optic of the excimer laser approximately 2 m from the center of the reaction cell, the beam was rectangular in cross section and measured 2.0 by 4.0 cm. When measured through a 0.5 cm diameter aperture, the fluence peaked at the center of the beam and dropped off by 10% per 0.5 cm distance from the center in both the vertical and horizontal directions. The beam from the Nd:YAG laser was aligned at the center of the volume irradiated by the excimer laser. It was estimated to be 0.4 ± 0.1 cm in diameter.

The reagent purities and sources were as follows: N_2 (99.999%, Spectra Gases, Inc.); Cl_2 (99.9%, Matheson Gas Products, Inc.); O_2 (99.99%, Spectra Gases, Inc.). Ozone was prepared in a commercial ozonator using UHP oxygen. It was stored at 195 K on silica gel and degassed at 77 K before use. The other gases were used without further purification.

RESULTS

In the absence of competing reactions that either deplete or enhance the ground state oxygen atom $[O(^3P)]$ concentration, the temporal behavior of $[O(^3P)]$ following the 266 nm laser pulse can be described by the relationship

$$\ln\{[O(^3P)]_t/[O(^3P)]_{t_d}\} = -(k_1[ClO] + k'_d)(t - t_d) = -k'(t - t_d), \quad \text{(I)}$$

where

$$k'_d = k_5[Cl_2] + k_6. \quad \text{(II)}$$

In Eq. (II), k_5 and k_6 are the rate coefficients for the following processes:

$$O(^3P) + Cl_2 \rightarrow \text{products}, \quad (5)$$

$$O(^3P) \rightarrow \text{loss by diffusion from the viewing zone and reaction with background impurities.} \quad (6)$$

A typical experimental $O(^3P)$ temporal profile is shown in Fig. 2. Unexpectedly, a significant buildup and decay of $O(^3P)$ occurred before the 266 nm laser fired; possible sources of this $O(^3P)$ and its implications for our study of reaction (1) are discussed below. It should be noted that the vertical axis in Fig. 2 has units of concentration. To construct Fig. 2, the fluorescence signal before the 266 nm laser fired was scaled to account for the fact that the 351 nm laser photolyzed the entire field of view of the detection system, while the 266 nm laser photolyzed only 15% of the detector viewing zone. The size of the viewing zone was estimated by placing a series of apertures in front of the 351 nm beam and noting the variation of fluorescence signal strength with beam size.

Typical decays of $O(^3P)$ generated by the 266 nm laser pulse are shown in Fig. 3. At each temperature and pressure a minimum of five and an average of eight experiments were performed at various values of $[O_3]_0$. Because the Nd:YAG laser fluence was measured in each experiment, the amount of ClO lost via 266 nm photolysis could be quantified. The expression

$$[ClO]_{t_d} = [O_3]_0 - [O(^3P)]_{t_d} \quad \text{(III)}$$

was used to calculate the ClO concentration under the as-

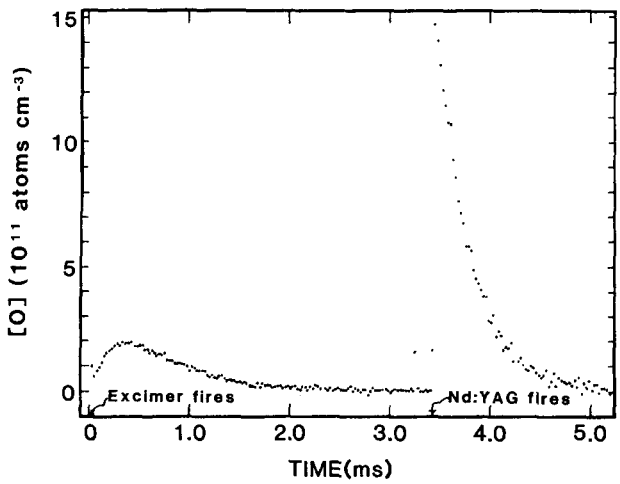

FIG. 2. An experimental O atom temporal profile obtained under the following conditions: $[Cl_2] = 1.40\times10^{16}$ molecules cm^{-3}; $[O_3]_0 = 7.27\times10^{13}$ molecules cm^{-3}; $[Cl]_0 = 1.82\times10^{14}$ molecules cm^{-3}; Total pressure = 25 Torr; temperature = 298 K; MCA dwell time = 25 μs.

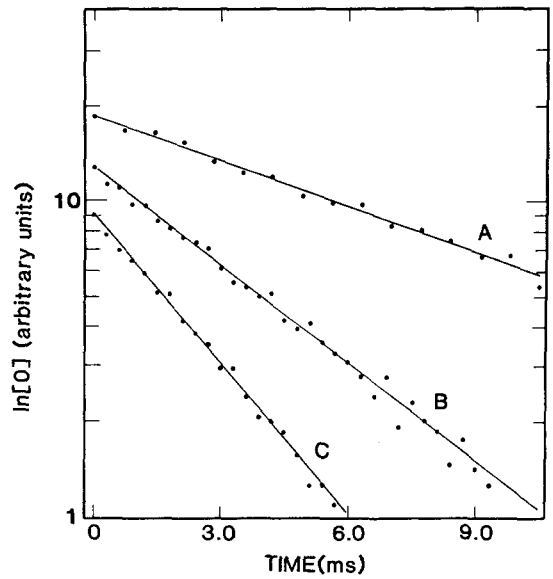

FIG. 3. Typical O atom temporal profiles. These experiments were carried out under the following conditions (all concentrations expressed in molecules cm^{-3}): 25 Torr total pressure; $T = 298$ K; $[Cl_2] = 9.8\times10^{15}$; $[O_3]_0 = 1.73\times10^{13}$ (A), 5.15×10^{13} (B), 8.76×10^{13} (C); and $[Cl]_0 = 1.10\times10^{14}$ (A); 1.66×10^{14} (B), 2.29×10^{14} (C).

sumption that no loss of ClO occurred during the delay between photolysis laser pulses. The ratio $[O(^3P)]/[ClO]$ immediately following the 266 nm laser pulse was determined for each experiment, and was typically in the range 0.01–0.04. Hence, it was appropriate to correct each measured decay rate for slight deviations from pseudo-first-order conditions. These corrections were derived from computer simulations of reactions (1), (5), and (6) under the range of experimental conditions employed. Best fit values for each decay rate (k') were obtained from linear regression analyses of the experimental data over at least 2 $1/e$ times. Each value of k' was then increased by 2% or less using the appropriate non-pseudo-first-order correction. Representative plots of [ClO] vs k' are shown in Fig. 4. These data were subjected to linear least squares analyses to give values for k_1. The results are presented in Table I. Note the separate columns for k_1(uncorrected) and k_1(corrected). The former represents the best fit to the data when k' was not corrected for non-pseudo-first-order behavior and [ClO] was set equal to $[O_3]_0$ less the amount photolyzed to produce $[O(^3P)]$. The latter k_1 values include the small non-pseudo-first-order correction to k' and additional corrections to [ClO] discussed below.

The absorption cross section used to calculate the amount of ClO photolyzed by the Nd:YAG laser was estimated experimentally. The signal level immediately after the Nd:YAG laser fired was directly proportional to the concentration of oxygen atoms. If the Nd:YAG laser was not preceded by a pulse from the excimer laser, then the photolyte was O_3. If all the O_3 had been converted to ClO via reaction with Cl atoms created in the 351 nm excimer pulse, then the signal was due to ClO photolysis. Therefore, in back-to-back experiments with constant $[Cl_2]$, $[O_3]$ and 266 nm fluence, the ratio of $O(^3P)$ signal with and without 351 nm photolysis should be identical to the ratio of the ClO and O_3 absorption

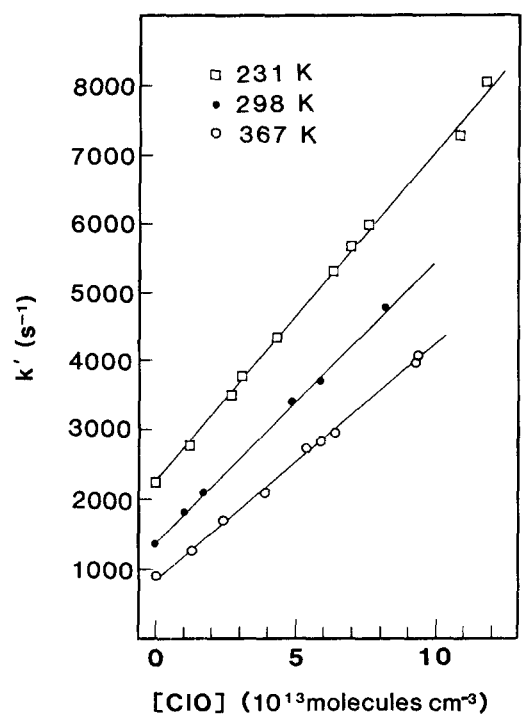

FIG. 4. A k' vs [ClO] plot of typical data taken at 25 Torr total pressure of N_2 and at three temperatures. Note that the 298 and 231 K data have been displaced upward by 1000 and 2000 s^{-1}, respectively. Solid lines are obtained from linear least squares analyses and give the following rate coefficients (in units of 10^{-11} cm^3 molecule^{-1} s^{-1}): 4.99 at 231 K, 4.07 at 298 K, 3.44 at 367 K.

TABLE I. Summary of k_1 determinations.[a]

Temperature (K)	Pressure (Torr)	$k_1\times10^{11}$ (uncorrected)[b] (cm^3 $molecule^{-1}$ s^{-1})	$k_1\times10^{11}$ (corrected) (cm^3 $molecule^{-1}$ s^{-1})
231	25	4.64 ± 0.16	4.99 ± 0.17
238	25	4.25 ± 0.43	4.47 ± 0.43
252	200	3.10 ± 0.22	3.97 ± 0.30
255	25	4.15 ± 0.20	4.42 ± 0.20
255	200	3.25 ± 0.20	3.95 ± 0.32
257	25	3.86 ± 0.15	4.10 ± 0.11
257	25	4.30 ± 0.15	4.47 ± 0.19
275	25	3.94 ± 0.17	4.10 ± 0.16
298	25	3.55 ± 0.21	3.84 ± 0.14
298	25	3.47 ± 0.25	3.59 ± 0.25
298	25	3.51 ± 0.14	3.62 ± 0.13
298	25	3.87 ± 0.36	3.93 ± 0.36
298	25	3.89 ± 0.15	4.07 ± 0.17
298	50	3.91 ± 0.23	4.07 ± 0.24
298	50	3.62 ± 0.15	3.98 ± 0.18
298	50	3.70 ± 0.12	3.91 ± 0.11[c]
298	50	3.53 ± 0.19	3.76 ± 0.14
298	50	3.76 ± 0.16	3.98 ± 0.14
298	100	3.73 ± 0.68	3.97 ± 0.67
298	200	3.39 ± 0.27	3.73 ± 0.24
298	200	3.39 ± 0.28	3.71 ± 0.32
298	200	3.55 ± 0.12	3.76 ± 0.13
298	500	3.18 ± 0.16	4.03 ± 0.20
338	25	3.16 ± 0.60	3.26 ± 0.12
359	200	2.99 ± 0.14	3.09 ± 0.15
360	25	2.89 ± 0.13	2.96 ± 0.12
367	25	3.35 ± 0.13	3.44 ± 0.13

[a] Errors are 2σ and represent precision only.
[b] Uncorrected values have not been adjusted for non-pseudo-first-order conditions and [ClO] loss by reaction (5). See the text for details.
[c] Carried out with 283 nm photolysis of ClO, under "reversed" and "normal" flow conditions.

cross sections at the Nd:YAG laser wavelength [the $O(^1D)$ product of O_3 photolysis is rapidly quenched to $O(^3P)$ by N_2]. This experiment resulted in a value of 0.35 for the signal ratio. If $\sigma_{266}(O_3)$ is taken to be 9.0×10^{-18} cm^2 (Ref. 13) then $\sigma_{266}(ClO)$ is $\sim3.1\times10^{-18}$ cm^2. This is somewhat lower than the low resolution cross section at this wavelength that is reported in the literature.[15] However, we carried out the identical signal level comparison near 283 nm, a wavelength where the high resolution cross section has been characterized.[16] Using a frequency doubled, Nd:YAG pumped tunable dye laser the rotational structure in the ClO spectrum was reproduced by observing the resonance fluorescence signal as the wavelength was scanned. At 282.95 nm, the peaks of the $R(19.5)$ and $P(16.5)$ lines of the $A\,^2\pi_{3/2}$–$X\,^2\pi_{3/2}$ 9–0 band, we observed a factor of 1.65 ± 0.20 more fluorescence signal when the excimer laser photolyzed Cl_2 than when the excimer laser beam was blocked. Based on the dye laser linewidth employed and the literature values for the ozone and ClO cross sections, we expected a ratio of 1.80 ± 0.40. This result confirms our value for $\sigma_{266}(ClO)$.

As mentioned above, the delay between the two laser pulses t_d, was adjusted to be long enough for reaction (2) to go to completion. The value of the $Cl+O_3$ rate constant is reasonably well known[13] so an appropriate delay time could be calculated. As a check the delay time was varied until a constant signal and decay rate were observed, indicating that all the O_3 had been converted to ClO. The majority of experiments were carried out with delay periods of either 3.4 or 6.4 ms.

The temporal behavior of ClO could be monitored by following both the $O(^3P)$ signal level produced by 266 nm photolysis and the measured value of k'. For some conditions (lower temperature, higher pressures) it was observed that ClO was decreasing on the time scale of the delay between the two lasers. The disappearance of ClO is probably due to self-reaction, a process that has not been completely characterized.[17] In order to make a correction for the amount of ClO lost during the delay between laser pulses and also during the O atom decay, a series of experiments were carried out in which the delay time was varied at fixed $[O_3]$, $[Cl_2]$, and laser fluences.

For the process

$$ClO + ClO \rightarrow \text{products} \qquad (7)$$

the time dependence of [ClO] is described by the relationship

$$2k_7t = [ClO]_t^{-1} - [ClO]_0^{-1}. \qquad (IV)$$

If we define k_7 to be the second-order rate coefficient for ClO removal under our experimental conditions, then plotting $[ClO]_t^{-1}$ vs t should yield a straight line of slope $2k_7$ and intercept equivalent to $[ClO]_0^{-1}$. The absolute concen-

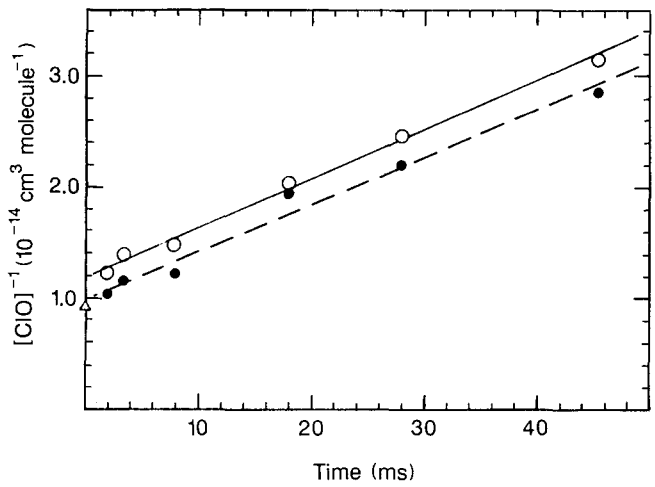

FIG. 5. A plot of $[ClO]^{-1}$ vs delay time. The open circles are based on ClO concentrations calculated from the O atom decay at each delay and the closed circles are based upon the fluorescence signal immediately following the 266 nm laser pulse. The triangular point on the abscissa represents $[O_3]_0^{-1}$. Experimental conditions: $T = 252$ K; $P = 200$ Torr.

tration of ClO needed to determine k_7 was deduced in two manners. In the first method, Eq. (I) was rearranged to calculate [ClO]. Here k_1 was taken from fixed delay experiments at the same experimental temperature and pressure. $k_{7'}$ was determined from Eq. (IV). Then the values for [ClO] in the fixed delay experiments were adjusted to account for the loss of ClO during the delay. This procedure was iterated until constant values of k_1 and $k_{7'}$ were obtained. The second method involved relating the signal level immediately following the 266 nm laser pulse to the value of [ClO]. The signal calibration could be arrived at by two procedures. When enough data was available under the same experimental conditions, a [ClO] vs signal calibration curve was constructed. Otherwise, signal vs delay time was plotted and extrapolated to time zero and that signal level normalized to $[O_3]_0$. This normalization factor was then used to put the signal level at each delay time on an absolute concentration scale. Because of the reciprocal relation in Eq. (IV), the value of $k_{7'}$ is quite sensitive to the scaling factor used in setting the value of [ClO]. Also the signal level is quite dependent on the operating conditions of the resonance lamp. Therefore, the values of $k_{7'}$ determined from the first method are more precise. However, when using k' as a measure of [ClO], we *assume* that O atoms are removed only by reaction with ClO and Cl_2; this assumption appears to be justified. A typical plot of $[ClO]^{-1}$ vs t appears in Fig. 5. The end results of a number of such experiments appear in Table II. These results are presented only as a measure of the phenomenological loss rate of ClO in our system, not as a definitive measurement of k_7.

Hayman *et al.*[17] report 298 K values for k_7 which are substantially faster than the values for $k_{7'}$ (298 K,P) we have determined. However, our 255 K results appear to agree reasonably well with Hayman *et al.*'s low temperature values for k_7. According to Hayman *et al.*,[17] reaction (7) has an important branch to form a weakly bound dimer which can either decompose or react rapidly with chlorine atoms. The relevant reaction scheme is given below:

$$ClO + ClO + M \leftrightarrow (ClO)_2 + M, \quad (7a, -7a)$$

$$ClO + ClO \rightarrow OClO + Cl, \quad (7b)$$

$$ClO + ClO \rightarrow \text{other products}, \quad (7c)$$

$$Cl + (ClO)_2 \rightarrow Cl_2 + ClOO, \quad (8)$$

$$ClOO + M \rightarrow Cl + O_2 + M, \quad (9)$$

$$Cl + ClOO \rightarrow Cl_2 + O_2 \text{ (major)}, \quad (10a)$$

$$Cl + ClOO \rightarrow 2ClO \text{ (minor)}, \quad (10b)$$

$$Cl + OClO \rightarrow 2ClO. \quad (11)$$

Hayman *et al.*[17] obtained their kinetic data from a molecular modulation study. They observed much smaller apparent values for k_7 during the lights-off cycle (no chlorine atoms present) than during the lights-on cycle (large concentration of chlorine atoms present). Hence, a plausible explanation for the difference between our $k_{7'}$ (298 K) determinations and the k_7 (298 K) values reported by Hayman *et al.*[17]

TABLE II. Summary of $k_{7'}$ determinations.

T(K)	P(Torr)	$10^{-14}[Cl]_0$ [a]	$10^{-13}[O_3]$ [a]	No. of experiments	Range of t_d (ms)	$10^{13}k_{7'}$ [b,c]
252	200	4.0–4.8	10.4	6	1.5–45	2.27 ± 0.18
255	25	4.0–5.1	9.8	6	3.0–45	0.47 ± 0.19
255	200	3.4–4.7	12.2	8	3.0–50	2.47 ± 0.18
298	16	1.7–2.5	7.3	7	1.5–60	0.17 ± 0.12
298	50	4.3–7.8	13.0	6	5.0–60	0.40 ± 0.09
298	50	2.2–5.2	8.3	8	1.5–60	0.36 ± 0.09
298	200	1.9–4.6	9.7	12	1.5–60	1.12 ± 0.11
298	200	2.6–3.9	6.15	6	1.5–60	0.92 ± 0.18
298	500	3.2–3.4	11.8	6	2.0–45	1.63 ± 0.17
298	500	3.7–4.0	5.9	5	1.5–35	2.94 ± 0.63
359	200	2.0–2.5	9.3	5	3.0–45	0.38 ± 0.15

[a] Units are molecules per cm^3.
[b] Units are cm^3 molecule^{-1} s^{-1}.
[c] Errors are 2σ, precision only.

TABLE III. Correction factors for loss of ClO via reaction (7) as a function of temperature, pressure, $[O_3]_0$, and $[Cl]_0/[O_3]_0$.

		255 K		298 K			363 K	
$[O_3]_0$	$[Cl]_0/[O_3]_0$ [a]	25 Torr	200 Torr	25 Torr[b]	200Torr	500 Torr	25 Torr	200 Torr
2.0×10^{13}	10	0.993	0.970	0.996	0.986	0.970	0.997	0.994
2.0×10^{13}	5	0.961	0.943	0.976	0.968	0.956	0.987	0.984
6.0×10^{13}	6	0.983	0.918	0.990	0.962	0.919	0.992	0.985
6.0×10^{13}	2	0.930	0.887	0.952	0.933	0.901	0.969	0.964
1.2×10^{14}	5	0.965	0.845	0.979	0.926	0.849	0.984	0.970
1.2×10^{14}	2	0.964	0.864	0.979	0.934	0.877	0.985	0.973

[a] Typical range of values for $[Cl]_0/[O_3]_0$ employed in k_1 determinations.
[b] $k_{7'}$ determined by interpolation to be 3×10^{-14} cm^3 molecule^{-1} s^{-1}.

is that $k_{-7a}(298\ K)$ was substantially faster than k_8 [Cl] under our experimental conditions, thus facilitating ClO regeneration by dimer decomposition; this is, of course, a favorable situation for measurement of k_1 but would result in systematic underestimation of k_7. No clear variation of $k_{7'}$ with [Cl] is evident in our data, although our experiments spanned a rather narrow range of chlorine atom concentrations (Table II).

In order to make appropriate corrections for the loss of ClO during the delay between laser pulses, a reaction system consisting of reactions (2) and (7) was modeled under a variety of initial conditions using literature values for $k_2(T)$[13] and setting $k_7 = k_{7'}$. From these calculations a set of correction factors (F) could be derived:

$$F_{t_d} = [ClO]_{t_d}/[O_3]_0. \qquad (V)$$

Values of F_{t_d} at $t_d = 3.4$ ms are given in Table III as a function of temperature, pressure, $[O_3]_0$, and $[Cl]_0/[O_3]_0$. Note that the maximum correction is made for the highest value of [ClO] for a given experiment; also, the longer the delay used in an experiment the larger the correction applied. For a few experimental conditions where $k_{7'}$ was great enough (i.e., high pressure, low temperature) a correction was made to the observed k' for loss of ClO during the decay itself; this correction never exceeded 1.4%.

As a further check on the consistency of our experiments, the rate coefficient for reaction (1) was determined at 298 K in 50 Torr N_2 using 283 nm photolysis of ClO rather than 266 nm photolysis. The additional photolysis wavelength was provided by the frequency doubled, Nd:YAG pumped tunable dye laser. Also, to ensure that neither O_3 nor Cl_2 were being lost in the flow system, a measurement of $k_1(298\ K)$ was carried out with the two absorption cells plumbed downstream from the reaction cell rather than in the "normal" upstream position. Neither of these variations in experimental parameters affected the observed kinetics.

As mentioned above, a significant O atom signal was generated subsequent to the excimer laser pulse (Fig. 2). Leu[4] and Vanderzanden and Birks[18] have observed O atoms from the reaction of chlorine atoms with ozone. The following chemistry was proposed to explain their observations:

$$Cl + O_3 \rightarrow ClO + O_2(b\ ^1\Sigma_g^+), \qquad (2')$$

$$O_2(b\ ^1\Sigma_g^+) + O_3 \rightarrow O + 2O_2. \qquad (12)$$

Subsequently, Choo and Leu[19] monitored $O_2(b\ ^1\Sigma_g^+)$ directly by observing its near infrared emission and put an upper limit of $\sim0.05\%$ on the $O_2(b\ ^1\Sigma_g^+)$ yield from reaction (2). Such a yield is much too small to account for the observed levels of $O(^3P)$ produced in the $Cl + O_3$ studies.[4,18] Choo and Leu have suggested that the O atoms may be generated by reactions of vibrationally excited ClO formed in reaction (2), i.e.,

$$Cl + O_3 \rightarrow ClO^*(v' \leqslant 18) + O_2, \qquad (2'')$$

followed by

$$ClO^*(v' \geqslant 12) + O_3 \rightarrow O_2 + O + ClO \qquad (13)$$

or

$$ClO^*(v' \geqslant 3) + Cl \rightarrow Cl_2 + O. \qquad (14)$$

In our system Cl atoms are in excess over O_3 and, therefore, in excess over the ClO created in reaction (2). Also, the occurence of reaction (14) results in loss of two ClO molecules which otherwise would have been present at t_d while the occurence of reaction (13) results in loss of only one ClO molecule. Hence, reaction (14) would potentially have the larger effect on the ClO concentration in our experiments. To examine the potential role of reaction (14) in consuming ClO, we simulated the system chemistry using a Gear routine to solve the rate equations numerically. The following scheme was modeled:

$$Cl + O_3 \rightarrow ClO^* + O_2, \qquad (2'')$$

$$Cl + ClO^* \rightarrow Cl_2 + O, \qquad (14)$$

$$ClO^* + M \rightarrow ClO + M(M = N_2), \qquad (15)$$

$$O + ClO \rightarrow O_2 + Cl, \qquad (1)$$

$$ClO + ClO \rightarrow \text{products}, \qquad (7')$$

$$O + Cl_2 \rightarrow ClO + Cl. \qquad (5a)$$

Although reactions (2") and (14) may have other channels, this scheme was devised to have the greatest impact on the [ClO] at the end of the reaction period; therefore, only the branches that deplete ClO were used. It should be noted that a large dependence of the extraneous $O(^3P)$ signal on the total pressure in the system was observed. This observation would be consistent with quenching of either ClO* or $O_2(b\ ^1\Sigma_g^+)$ by N_2. k_1 and k_5 are known, and the other rate coefficients were adjusted to reproduce the magnitude and

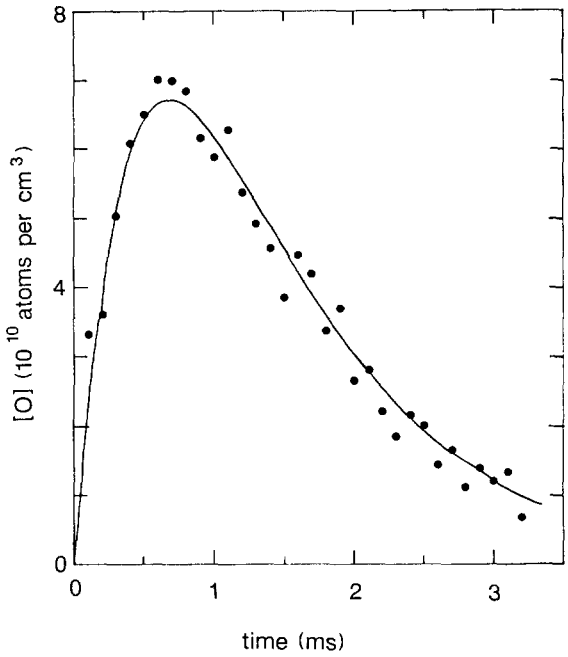

FIG. 6. Comparison of oxygen atom temporal profile immediately following 351 nm laser pulse to computer simulation of reaction scheme discussed in the text. Experimental conditions are as follows: $T = 298$ K; $[O_3]_0 = 1.65\times10^{13}$ molecules cm^{-3}; $[Cl_2] = 1.42\times10^{16}$ molecules cm^{-3}; $[Cl]_0 = 1.81\times10^{14}$ molecules cm^{-3}; pressure = 25 Torr. The reaction rate coefficients used in the simulation are: $k_1 = 3.66\times10^{-11}$; $k_{2'} = 1.18\times10^{-11}$; $k_5 = 2.91\times10^{-14}$; $k_{7'} = 3.0\times10^{-14}$; $k_{13} = 2.0\times10^{-11}$; $k_{14} = 5.8\times10^{-13}$. All rate coefficients are in units of cm^3 $molecule^{-1}$ s^{-1}.

temporal behavior of the O atom signal observed. Typical results are shown in Fig. 6. It was found that the above reaction scheme lead to no more than a 2% perturbation in the concentration of ClO. Of course there is no direct proof that the assumed reaction scheme is correct. However, it is the worst case of the suggested possibilities and any corrections would be quite small. Since the mechanism for O atom formation following the excimer laser pulse is not well understood, the effect of this chemistry on the ClO concentration was not taken into account in the determination of "corrected" values for k_1 (Table I).

The combination of Cl_2 photolysis, $Cl + O_3$ reaction, and ClO photolysis could result in some heating of the gas in the reaction zone. Calculations which assume worst case conditions, i.e., $P = 25$ Torr N_2, $[Cl]_0 = 6\times10^{14}$ molecules per cm^3, $[O_3]_0 = 1\times10^{14}$ molecules per cm^3, $[O]_{t_d} = 2\times10^{12}$ atoms per cm^3, and all excess energy dissipated as heat show that laser heating of the reaction zone could not have exceeded 2 K in any experiment. This potential systematic error is negligibly small so it was not incorporated into the data analysis.

As discussed above, several corrections were made to either the observed k' values or in the calculation of [ClO] from $[O_3]_0$. For clarity this set of corrections is reiterated:

(a) A quantitative correction was made in k' for non-pseudo-first-order conditions during the O atom decay. In only a few cases did this exceed a 1% adjustment.

(b) [ClO] was corrected for the amount of ClO lost to photolysis at 266 nm. This correction was dependent upon knowledge of the laser fluence, which was monitored in every experiment using a calibrated radiometer, and on our estimated value of $\sigma_{266}(ClO)$. Because there was only a small adjustment to [ClO] (on the average 3%) the final results were not very sensitive to this correction. For example, in an experiment where the fraction of ClO photolyzed was above the average, an increase in $\sigma_{266}(ClO)$ of a factor of 2 was found to change the final value of k_1 by only 4%.

(c) Using the loss rate of ClO determined in the same system, a correction was made to [ClO] for the ClO that undergoes self-reaction (or other loss processes) during the delay time between laser firings. The largest corrections were made at higher pressures, lower temperatures, and in long delay experiments. Because the simulation of the production and loss of ClO was sensitive to the errors in our measurements of $k_{7'}$, this correction has a rather large uncertainty.

(d) A few decays were corrected for ClO loss during the decay itself; however, this correction was insignificant under most experimental conditions.

(e) It was concluded that of the known possibilities for the source of O atoms prior to ClO photolysis, none could have had more than a 2% effect on $[ClO]_{t_d}$; no corrections were made for this chemistry.

Even though there were several corrections made in order to reach a final value for k_1 at each temperature and pressure, the magnitudes of the corrections were small in most cases (see Table I), the corrections could be quantitatively applied, and in general, the results are self-consistent. An Arrhenius plot of our data appears in Fig. 7. An unweighted least squares analysis of all data yields the expression

$$k_1(T) = (1.68 \pm 0.31)\times10^{-11}\exp\{(241 \pm 53)/T\}$$
$$cm^3\ molecule^{-1}\ s^{-1}, \qquad \text{(VI)}$$

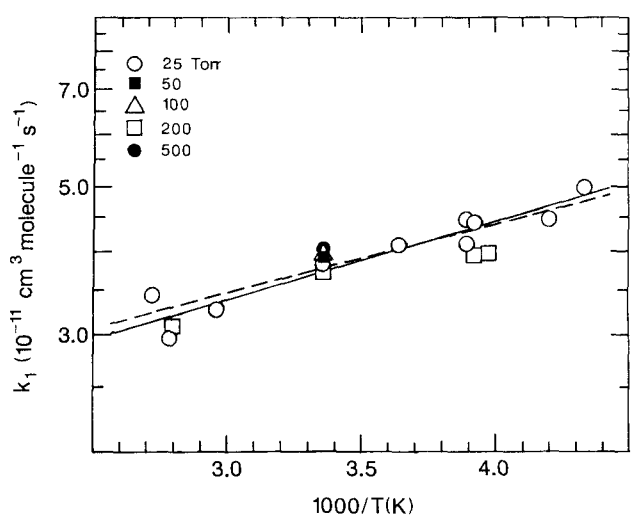

FIG. 7. Arrhenius plot of our results for $k_1(T,P)$. The dashed line represents an unweighted least squares analysis of the 25 Torr data only while the solid line includes all data.

where the errors represent 2σ, precision only, and $\sigma_A \equiv A\sigma_{\ln A}$. For the 25 Torr data only, the expression

$$k_1(T) = (1.55 \pm 0.33)\times 10^{-11} \exp\{(263 \pm 60)/T\}$$
$$\text{cm}^3 \text{ molecule}^{-1} \text{ s}^{-1} \qquad \text{(VII)}$$

is obtained from an unweighted least squares analysis. The difference between the Arrhenius expression obtained from the 25 Torr data and that obtained from the complete data set is primarily due to the slightly lower rate coefficients obtained at high pressure (200 Torr) and low temperature (252–255 K). These rate coefficients required rather large corrections for contributions from reaction (7) and, therefore, are more likely to be in error than rate coefficients obtained at higher temperatures and/or lower pressures. For this reason, we believe the Arrhenius expression obtained from the 25 Torr data only should be preferred. The absolute accuracy of k_1 at any temperature within the range studied is estimated to be $\pm 20\%$.

DISCUSSION

In all prior investigations, reaction (1) was studied by flow tube techniques at pressures less than 10 Torr. The results of all studies are summarized in Table IV. In the earliest study Bemand *et al.*,[1] measured $k_1(298\text{ K})$ using resonance fluorescence to monitor $O(^3P)$ in excess ClO. The ClO was produced by the reaction

$$Cl + OClO \rightarrow 2ClO \qquad (11)$$

assuming a stoichiometric factor of 2. These workers reported $k_1(298\text{ K}) = (5.3 \pm 0.8)\times 10^{-11}$ cm^3 molecule^{-1} s^{-1}. They also measured the rate coefficient by following the decay of ClO mass spectrometrically in excess oxygen atoms and obtained the result $(5.7 \pm 2.3)\times 10^{-11}$ cm^3 molecule^{-1} s^{-1}. In a subsequent study in the same laboratory Clyne and Nip[2] measured the temperature dependence of k_1. Again, $O(^3P)$ was monitored by resonance fluorescence in excess ClO, the latter species being generated via reaction (2). The room temperature rate coefficient was in good agreement with their previous study. They report a significant activation energy and quote the Arrhenius expression $k_1(T) = (1.07 \pm 0.30)\times 10^{-10} \exp\{-(224 \pm 76)/T\}$ cm^3 molecule^{-1} s^{-1}.

Zahniser and Kaufman[3] measured the temperature dependence of the ratio k_1/k_2. Using a value of k_2 measured directly in the same system these workers report $k_1(T) = (3.38 \pm 0.50)\times 10^{-11} \exp\{(75 \pm 40)/T\}$ cm^3 molecule^{-1} s^{-1}.

The next reported investigation of $k_1(T)$ was performed by Leu[4] using resonance fluorescence detection of $O(^3P)$ in excess ClO. ClO radicals were produced using three different source reactions in order to validate stoichiometric assumptions necessary to arrive at ClO concentration levels. Reactions (2), (11), and

$$Cl + Cl_2O \rightarrow ClO + Cl_2 \qquad (16)$$

were the three sources used at room temperature. Reaction (2) was used at all other temperatures. Leu's value for $k_1(298)$ is lower than the previously reported values and he measured a small positive activation energy with $k_1(T) = (5.0 \pm 1.0)\times 10^{-11} \exp\{-(96 \pm 20)/T\}$ cm^3 molecule^{-1} s^{-1}. The use of reaction (2) as the only ClO source in all experiments at $T \neq 298$ K could result in a systematic error in Leu's reported temperature dependence. At the low pressures employed in Leu's study, the ClO* + Cl reaction may have competed favorably with ClO* deactivation, thus leading to overestimation of [ClO]. Since the ratio of k_{14}/k_{15} may be temperature dependent, such an effect could have been more important at one end of the investigated temperature range than at the other end. It should be emphasized that while the abovementioned systematic error in Leu's [ClO] determination is possible, there currently exists insufficient information concerning ClO* chemistry to prove or disprove this conjecture.

TABLE IV. Comparison of measurements of k_1.

Investigators	Reference	Experimental method[a,b]	Temperture range (K)	Pressure range (Torr)	$k_1(10^{-11}$ cm^3 molecule^{-1} s$^{-1})$[c] 210 K	250 K	298 K
Bemand, Clyne, and Watson	1	DF-RF(O)	298	~1.0	···	···	5.3 ± 0.8
	1	DF-MS(ClO)	298	0.75	···	···	5.7 ± 2.3
Clyne and Nip	2	DF-RF(O)	220–426	0.90	3.68	4.37	5.05
Zahniser and Kaufman	3	DF-RF(Cl)[d]	220–298	2.0–4.0	4.83	4.56	4.35
Leu	4	DF-RF(O)	236–422	1.0–3.5	3.17	3.41	3.62
Schwab, Toohey, Brune, and Anderson	5	DF-LMR(ClO) DF-RF(O)	252–347	0.8–2.0	3.50	3.50	3.50
Ongstad and Birks	6	DF-CL(O)[e]	220–387	2.3	4.14	3.85	3.61
Margitan	7	DF-LFP-RF(O)	241–298	10	4.20	4.20	4.20
Nicovich, Wine, and Ravishankara	This work	LFP-RF(O)	231–367	25–500	5.29	4.41	3.77
				25	5.42	4.44	3.75

[a] DF—discharge flow; RF—resonance fluorescence; MS—mass spectrometry; LMR—laser magnetic resonance; CL—chemiluminescence; LFP—laser flash photolysis.
[b] The monitored species is given in parentheses.
[c] Calculated from reported Arrhenius expressions.
[d] $k(O + ClO)$ measured relative to $k(Cl + O_3)$.
[e] NO added to produce chemiluminescence via $O + NO + M \rightarrow NO_2^* \rightarrow h\nu + NO_2$.

Schwab *et al.*[5] employed an experimental apparatus in which both reactants [ClO by laser magnetic resonance and $O(^3P)$ by resonance fluorescence] and one product (Cl atoms by resonance fluorescence) could be monitored. [Interestingly, this is the only O + ClO study where ClO was directly measured in the reaction zone.] Again, a somewhat lower value was measured [$k_1(298\ \text{K}) = (3.5 \pm 0.5) \times 10^{-11}$ cm^3 molecule^{-1} s^{-1}) and these workers observed essentially no temperature dependence for k_1.

Ongstad and Birks[6] measured $k_1(T)$ in a discharge flow system using the same three sources of ClO as Leu.[4] $O(^3P)$ was followed via the chemiluminescence from NO_2^* generated by reacting the oxygen atoms with NO added to the detection region of their flow tube. These workers measured $k_1(T)$ directly and also relative to the reaction

$$O + NO_2 \rightarrow NO + O_2. \quad (17)$$

In a successive measurement scheme $k_{17}(T)$ was also measured. The relative measurements yielded somewhat higher values, presumably due to nonpure source gases (Cl_2O, ClO_2, O_3) or other channels for the source reactions. Ongstad and Birks measured a value for $k_1(298\ \text{K})$ that agrees with the other more recent studies and a small "negative activation energy." They reported the expression $k_1(T) = (2.61 \pm 0.60) \times 10^{-11} \exp\{(97 \pm 64)/T\}$ cm^3 molecule^{-1} s^{-1}.

The only other study of k_1 at or near room temperature reported in the literature was by Margitan.[7] ClO radicals were generated in a flow tube via reaction (16). Downstream from this source $O(^3P)$ was created by laser photolysis of the ClO and followed by resonance fluorescence. The ClO concentration was measured directly in the flow by absorption. However, large corrections (up to 20%) had to be made for ClO loss between the ClO detection region and the $O(^3P)$ detection region. Margitan used literature values for k_7 to make these corrections. Given the recent advances in our understanding of reaction (7),[17] a large uncertainty must be associated with the magnitude of Margitan's correction for ClO loss via the self-reaction. His results are also very dependent on the value chosen for the ClO absorption cross section. Margitan reports that E/R lies within the range ± 200 K and $k_1(298\ \text{K}) = (4.2 \pm 0.8) \times 10^{-11}$ cm^3 molecule^{-1} s^{-1}.

As seen by the comparison in Table IV, there is very little difference between the value of $k_1(298\ \text{K})$ from our experiments and from any of the other recent studies. However, at the lower temperatures typical of the middle stratosphere our results indicate significantly faster values for $k_1(T)$ than any of the other recent investigations (see Table IV). Hence, model calculations which employ our expression for $k_1(T)$ would predict somewhat larger ozone depletion due to chlorofluorocarbon injection than calculations which take $k_1(T)$ from previously available data.

SUMMARY

We have measured k_1 as a function of temperature and pressure. Our results indicate a lack of any pressure dependence at 298 K over the range 25 to 500 Torr. Although our 298 K rate coefficient agrees well with previous studies, our observation of an activation energy that is more negative than any previously reported leads to a significant difference between our result and other recent measurements at temperatures relevant to stratospheric chemistry.

ACKNOWLEDGMENTS

We thank M. McQuaid for carrying out some of the computer simulations. This work was supported by the fluorocarbon program panel of the Chemical Manufacturer's Association (Contract No. FC-84-499) and by the National Aeronautics and Space Administration (Grant No. NAGW-1001).

[1] P. P. Bemand, M. A. A. Clyne, and R. T. Watson, J. Chem. Soc. Faraday Trans. 1 **69**, 1356 (1973).
[2] M. A. A. Clyne and W. S. Nip, J. Chem. Soc. Faraday Trans. 1 **72**, 2211 (1976).
[3] M. S. Zahniser and F. Kaufman, J. Chem. Phys. **66**, 3673 (1977).
[4] M. T. Leu, J. Phys. Chem. **88**, 1394 (1984).
[5] J. J. Schwab, D. W. Toohey, W. H. Brune, and J. G. Anderson, J. Geophys. Res. **89**, 9581 (1984).
[6] (a) A. P. Ongstad and J. W. Birks, J. Chem. Phys. **81**, 3922 (1984); (b) **85**, 3359 (1986).
[7] J. J. Margitan, J. Phys. Chem. **88**, 3639 (1984).
[8] C. Park, J. Phys. Chem. **80**, 565 (1976).
[9] R. L. Jaffee, Chem. Phys. **40**, 185 (1979).
[10] J. L. Gole, J. Phys. Chem. **84**, 1333 (1980).
[11] A. R. Ravishankara, P. H. Wine, and J. M. Nicovich, J. Chem. Phys. **78**, 6629 (1983).
[12] J. M. Nicovich and P. H. Wine, J. Phys. Chem. **91**, 5118 (1987).
[13] W. B. Demore, M. J. Molina, S. P. Sander, D. M. Golden, R. F. Hampson, M. J. Kurylo, C. J. Howard, and A. R. Ravishankara, JPL Publication 87-41, 1987.
[14] (a) A. G. Hearn, Proc. Phys. Soc. **78**, 932 (1961). (b) L. T. Molina and M. J. Molina, J. Geophys. Res. **91**, 14501 (1986). (c) K. Mauersberger, J. Barnes, D. Hanson, and J. Morton, Geophys. Res. Lett. **13**, 671 (1986).
[15] M. Mandelman and R. W. Nicholls, J. Quant. Spectrosc. Radiat. Transfer **17**, 483 (1977).
[16] P. H. Wine, A. R. Ravishankara, D. L. Philen, D. D. Davis, and R. T. Watson, Chem. Phys. Lett. **50**, 101 (1977).
[17] G. D. Hayman, J. M. Davies, and R. A. Cox, Geophys. Res. Lett. **13**, 1347 (1986).
[18] J. W. Vanderzanden and J. W. Birks, Chem. Phys. Lett. **88**, 109 (1982).
[19] K. Y. Choo and M. T. Leu, J. Phys. Chem. **89**, 4832 (1985).